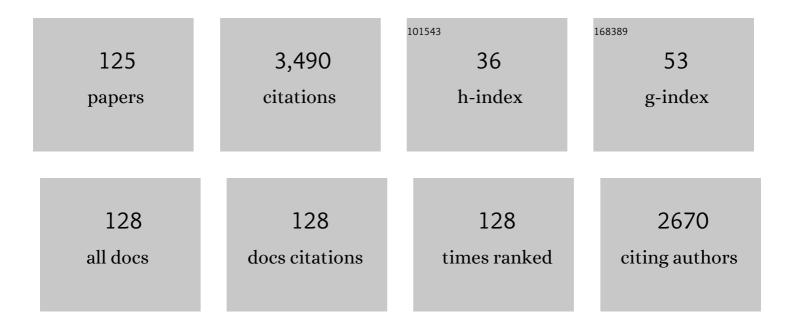
Muhammad Bilal

List of Publications by Year in descending order

Source: https://exaly.com/author-pdf/7670704/publications.pdf Version: 2024-02-01



ΜΠΗΛΜΜΛΟ ΒΙΙΛΙ

#	Article	IF	CITATIONS
1	Thick Clouds Removing From Multitemporal Landsat Images Using Spatiotemporal Neural Networks. IEEE Transactions on Geoscience and Remote Sensing, 2022, 60, 1-14.	6.3	14
2	Uncertainty in Aqua-MODIS Aerosol Retrieval Algorithms During COVID-19 Lockdown. IEEE Geoscience and Remote Sensing Letters, 2022, 19, 1-5.	3.1	8
3	Edge Task Migration With 6C-Enabled Network in Box for Cybertwin-Based Internet of Vehicles. IEEE Transactions on Industrial Informatics, 2022, 18, 4893-4901.	11.3	7
4	Biodegradation of environmental pollutants using horseradish peroxidase. , 2022, , 603-633.		1
5	Evaluation and comparison of MODIS and VIIRS aerosol optical depth (AOD) products over regions in the Eastern Mediterranean and the Black Sea. Atmospheric Environment, 2022, 268, 118784.	4.1	15
6	Evaluation and comparison of CMIP6 models and MERRA-2 reanalysis AOD against Satellite observations from 2000 to 2014 over China. Geoscience Frontiers, 2022, 13, 101325.	8.4	25
7	Study on Vertically Distributed Aerosol Optical Characteristics over Saudi Arabia Using CALIPSO Satellite Data. Applied Sciences (Switzerland), 2022, 12, 603.	2.5	1
8	Integration of Surface Reflectance and Aerosol Retrieval Algorithms for Multi-Resolution Aerosol Optical Depth Retrievals over Urban Areas. Remote Sensing, 2022, 14, 373.	4.0	11
9	Impacts of aerosols and climate modes on tropical cyclone frequency over the North Indian Ocean: a statistical link approach. Journal of Climate, 2022, , 1-46.	3.2	Ο
10	Spatio-Temporal Characteristics of Air Quality Index (AQI) over Northwest China. Atmosphere, 2022, 13, 375.	2.3	13
11	PM2.5 Concentration Exposure over the Belt and Road Region from 2000 to 2020. International Journal of Environmental Research and Public Health, 2022, 19, 2852.	2.6	8
12	A dark target Kalman filter algorithm for aerosol property retrievals in urban environment using multispectral images. Urban Climate, 2022, 43, 101135.	5.7	7
13	A Multiscale Land Use Regression Approach for Estimating Intraurban Spatial Variability of PM2.5 Concentration by Integrating Multisource Datasets. International Journal of Environmental Research and Public Health, 2022, 19, 321.	2.6	4
14	Editorial: Impact of climate change on hydrology and water resources. Journal of Water and Climate Change, 2022, 13, 3-vi.	2.9	2
15	Spatiotemporal changes in aerosols over Bangladesh using 18 years of MODIS and reanalysis data. Journal of Environmental Management, 2022, 315, 115097.	7.8	11
16	Spatiotemporal Investigation of Near-Surface CO ₂ and Its Affecting Factors Over Asia. IEEE Transactions on Geoscience and Remote Sensing, 2022, 60, 1-16.	6.3	9
17	Long-Time Variation and Mechanism of Surface Energy Budget Over Diverse Geographical Regions in Pakistan. IEEE Journal of Selected Topics in Applied Earth Observations and Remote Sensing, 2022, 15, 5203-5213.	4.9	2
18	Unprecedented environmental and energy impacts and challenges of COVID-19 pandemic. Environmental Research, 2021, 193, 110443.	7.5	73

#	Article	IF	CITATIONS
19	Evaluation of atmospheric correction methods for low to high resolutions satellite remote sensing data. Atmospheric Research, 2021, 249, 105308.	4.1	23
20	A High-Precision Aerosol Retrieval Algorithm (HiPARA) for Advanced Himawari Imager (AHI) data: Development and verification. Remote Sensing of Environment, 2021, 253, 112221.	11.0	58
21	Remote sensing estimation of phytoplankton absorption associated with size classes in coastal waters. Ecological Indicators, 2021, 121, 107198.	6.3	3
22	Phytoplankton "Missing―Absorption in Marine Waters: A Novel Pigment Compensation Model for the Packaging Effect. Journal of Geophysical Research: Oceans, 2021, 126, .	2.6	3
23	Ground-Based MAX-DOAS Observations of Tropospheric NO2 and HCHO During COVID-19 Lockdown and Spring Festival Over Shanghai, China. Remote Sensing, 2021, 13, 488.	4.0	28
24	Urban Pollution. Urban Book Series, 2021, , 243-258.	0.6	0
25	Spatiotemporal Investigations of Multi-Sensor Air Pollution Data over Bangladesh during COVID-19 Lockdown. Remote Sensing, 2021, 13, 877.	4.0	32
26	Spatio-Temporal Characteristics of PM2.5, PM10, and AOD over the Central Line Project of China's South-North Water Diversion in Henan Province (China). Atmosphere, 2021, 12, 225.	2.3	4
27	Validation of GOSAT and OCO-2 against In Situ Aircraft Measurements and Comparison with CarbonTracker and GEOS-Chem over Qinhuangdao, China. Remote Sensing, 2021, 13, 899.	4.0	22
28	Utilizing world urban database and access portal tools (WUDAPT) and machine learning to facilitate spatial estimation of heatwave patterns. Urban Climate, 2021, 36, 100797.	5.7	10
29	Performance of MODIS C6.1 Dark Target and Deep Blue aerosol products in Delhi National Capital Region, India: Application for aerosol studies. Atmospheric Pollution Research, 2021, 12, 65-74.	3.8	17
30	Climatic Change and Human Activities Link to Vegetation Dynamics in the Aral Sea Basin Using NDVI. Earth Systems and Environment, 2021, 5, 303-318.	6.2	19
31	Remote Sensing Indices for Spatial Monitoring of Agricultural Drought in South Asian Countries. Remote Sensing, 2021, 13, 2059.	4.0	51
32	Automatic mapping of urban green spaces using a geospatial neural network. GIScience and Remote Sensing, 2021, 58, 624-642.	5.9	22
33	WRF-Chem Simulation for Modeling Seasonal Variations and Distributions of Aerosol Pollutants over the Middle East. Remote Sensing, 2021, 13, 2112.	4.0	6
34	Aerosol characteristics from earth observation systems: A comprehensive investigation over South Asia (2000–2019). Remote Sensing of Environment, 2021, 259, 112410.	11.0	60
35	Recommendations for HCHO and SO2 Retrieval Settings from MAX-DOAS Observations under Different Meteorological Conditions. Remote Sensing, 2021, 13, 2244.	4.0	5
36	Spatio-temporal Investigations of Monsoon Precipitation and Its Historical and Future Trend over Sudan. Earth Systems and Environment, 2021, 5, 519-529.	6.2	6

#	Article	IF	CITATIONS
37	Identification of Aerosol Pollution Hotspots in Jiangsu Province of China. Remote Sensing, 2021, 13, 2842.	4.0	11
38	Spatiotemporal variations and long term trends analysis of aerosol optical depth over the United Arab Emirates. Remote Sensing Applications: Society and Environment, 2021, 23, 100532.	1.5	0
39	Comparison of Multi-Year Reanalysis, Models, and Satellite Remote Sensing Products for Agricultural Drought Monitoring over South Asian Countries. Remote Sensing, 2021, 13, 3294.	4.0	50
40	Spatiotemporal variability of rainfall trends and influencing factors in Rwanda. Journal of Atmospheric and Solar-Terrestrial Physics, 2021, 219, 105631.	1.6	17
41	Identification of NO2 and SO2 Pollution Hotspots and Sources in Jiangsu Province of China. Remote Sensing, 2021, 13, 3742.	4.0	18
42	Air pollution scenario over Pakistan: Characterization and ranking of extremely polluted cities using long-term concentrations of aerosols and trace gases. Remote Sensing of Environment, 2021, 264, 112617.	11.0	79
43	Reduction of surface radiative forcing observed from remote sensing data during global COVID-19 lockdown. Atmospheric Research, 2021, 261, 105729.	4.1	6
44	MODIS high-resolution MAIAC aerosol product: Global validation and analysis. Atmospheric Environment, 2021, 264, 118684.	4.1	42
45	Spatio-Temporal Trends of Surface Energy Budget in Tibet from Satellite Remote Sensing Observations and Reanalysis Data. Remote Sensing, 2021, 13, 256.	4.0	16
46	Comparison Between SREM and 6SV Atmospheric Correction Methods. , 2021, , .		0
47	Flood Mitigation in the Transboundary Chenab River Basin: A Basin-Wise Approach from Flood Forecasting to Management. Remote Sensing, 2021, 13, 3916.	4.0	9
48	Summer monsoon rainfall variations and its association with atmospheric circulations over Sudan. Journal of Atmospheric and Solar-Terrestrial Physics, 2021, 225, 105751.	1.6	4
49	Neural-network-based estimation of regional-scale anthropogenic CO ₂ emissions using an Orbiting Carbon Observatory-2 (OCO-2) dataset over East and West Asia. Atmospheric Measurement Techniques, 2021, 14, 7277-7290.	3.1	25
50	Object-based multi-modal convolution neural networks for building extraction using panchromatic and multispectral imagery. Neurocomputing, 2020, 386, 136-146.	5.9	15
51	Thick Clouds Removal From Multitemporal ZY-3 Satellite Images Using Deep Learning. IEEE Journal of Selected Topics in Applied Earth Observations and Remote Sensing, 2020, 13, 143-153.	4.9	33
52	Effects of land use and cultivation histories on the distribution of soil organic carbon stocks in the area of the Northern Nile Delta in Egypt. Carbon Management, 2020, 11, 341-354.	2.4	5
53	Classification of aerosols over Saudi Arabia from 2004–2016. Atmospheric Environment, 2020, 241, 117785.	4.1	41
54	Turbidity Estimation from GOCI Satellite Data in the Turbid Estuaries of China's Coast. Remote Sensing, 2020, 12, 3770.	4.0	12

Muhammad Bilal

#	Article	IF	CITATIONS
55	Multi-Year Comparison of CO2 Concentration from NOAA Carbon Tracker Reanalysis Model with Data from GOSAT and OCO-2 over Asia. Remote Sensing, 2020, 12, 2498.	4.0	27
56	Climatic Characteristics and Modeling Evaluation of Pan Evapotranspiration over Henan Province, China. Land, 2020, 9, 229.	2.9	3
57	An Investigation of Vertically Distributed Aerosol Optical Properties over Pakistan Using CALIPSO Satellite Data. Remote Sensing, 2020, 12, 2183.	4.0	16
58	Comparison of MODIS- and CALIPSO-Derived Temporal Aerosol Optical Depth over Yellow River Basin (China) from 2007 to 2015. Earth Systems and Environment, 2020, 4, 535-550.	6.2	15
59	Statistical Approach to Observe the Atmospheric Density Variations Using Swarm Satellite Data. Atmosphere, 2020, 11, 897.	2.3	4
60	Estimating PM2.5 Concentrations Using Spatially Local Xgboost Based on Full-Covered SARA AOD at the Urban Scale. Remote Sensing, 2020, 12, 3368.	4.0	18
61	Spatio-Temporal Characteristics of PM2.5, PM10, and AOD over Canal Head Taocha Station, Henan Province. Remote Sensing, 2020, 12, 3432.	4.0	6
62	A novel water body extraction neural network (WBE-NN) for optical high-resolution multispectral imagery. Journal of Hydrology, 2020, 588, 125092.	5.4	39
63	Estimation of Hourly Ground-Level PM2.5 Concentration Based on Himawari-8 Apparent Reflectance. IEEE Transactions on Geoscience and Remote Sensing, 2020, , 1-10.	6.3	14
64	Estimation of High-Resolution PM _{2.5} over the Indo-Gangetic Plain by Fusion of Satellite Data, Meteorology, and Land Use Variables. Environmental Science & Technology, 2020, 54, 7891-7900.	10.0	77
65	Optical and Physical Characteristics of Aerosol Vertical Layers over Northeastern China. Atmosphere, 2020, 11, 501.	2.3	14
66	Constructing a gridded direct normal irradiance dataset in China during 1981–2014. Renewable and Sustainable Energy Reviews, 2020, 131, 110004.	16.4	15
67	First Experiences with the Landsat-8 Aquatic Reflectance Product: Evaluation of the Regional and Ocean Color Algorithms in a Coastal Environment. Remote Sensing, 2020, 12, 1938.	4.0	8
68	Air Pollution Scenario over China during COVID-19. Remote Sensing, 2020, 12, 2100.	4.0	68
69	Urbanization and regional air pollution across South Asian developing countries – A nationwide land use regression for ambient PM2.5 assessment in Pakistan. Environmental Pollution, 2020, 266, 115145.	7.5	54
70	Remote sensing of water turbidity in the Eastern China Seas from Geostationary Ocean Colour Imager. International Journal of Remote Sensing, 2020, 41, 4080-4101.	2.9	8
71	Cloud and Cloud Shadow Detection Based on Multiscale 3D-CNN for High Resolution Multispectral Imagery. IEEE Access, 2020, 8, 16505-16516.	4.2	14
72	Aerosol Optical Properties and Contribution to Differentiate Haze and Haze-Free Weather in Wuhan City. Atmosphere, 2020, 11, 322.	2.3	5

#	Article	IF	CITATIONS
73	HEAD: a robust high-resolution satellite image-based aerosol optical depth retrieval algorithm in the blue wavelength range using Kalman filters. , 2020, , .		1
74	Evaluation of the Aqua-MODIS C6 and C6.1 Aerosol Optical Depth Products in the Yellow River Basin, China. Atmosphere, 2019, 10, 426.	2.3	6
75	Optical and Physical Characteristics of the Lowest Aerosol Layers over the Yellow River Basin. Atmosphere, 2019, 10, 638.	2.3	7
76	Characteristics of Fine Particulate Matter (PM2.5) over Urban, Suburban, and Rural Areas of Hong Kong. Atmosphere, 2019, 10, 496.	2.3	22
77	Long-term spatiotemporal variations of aerosol optical depth over Yellow and Bohai Sea. Environmental Science and Pollution Research, 2019, 26, 7969-7979.	5.3	14
78	Variability of the Suspended Particle Cross-Sectional Area in the Bohai Sea and Yellow Sea. Remote Sensing, 2019, 11, 1187.	4.0	2
79	A Simplified and Robust Surface Reflectance Estimation Method (SREM) for Use over Diverse Land Surfaces Using Multi-Sensor Data. Remote Sensing, 2019, 11, 1344.	4.0	58
80	Aerosol optical depth climatology over Central Asian countries based on Aqua-MODIS Collection 6.1 data: Aerosol variations and sources. Atmospheric Environment, 2019, 207, 205-214.	4.1	58
81	Evaluation of Terra-MODIS C6 and C6.1 Aerosol Products against Beijing, XiangHe, and Xinglong AERONET Sites in China during 2004-2014. Remote Sensing, 2019, 11, 486.	4.0	39
82	High-Resolution Satellite Image Based Aerosol Optical Depth Retrieval Method: Validation Through EARLINET and NASA MPLNET Lidar Measurements and NASA AERONET Sunphotometer Data. , 2019, , .		1
83	PM2.5 mapping using integrated geographically temporally weighted regression (GTWR) and random sample consensus (RANSAC) models. Environmental Science and Pollution Research, 2019, 26, 1902-1910.	5.3	21
84	Mapping daily PM2.5 at 500†m resolution over Beijing with improved hazy day performance. Science of the Total Environment, 2019, 659, 410-418.	8.0	16
85	Synoptic relationships to estimate phytoplankton communities specific to sizes and species from satellite observations in coastal waters. Optics Express, 2019, 27, A1156.	3.4	4
86	Potential of VIS-NIR spectroscopy to characterize and discriminate topsoils of different soil types in the Triffa plain (Morocco). Soil Science Annual, 2019, 70, 54-63.	0.8	9
87	Influences of socioeconomic vulnerability and intra-urban air pollution exposure on short-term mortality during extreme dust events. Environmental Pollution, 2018, 235, 155-162.	7.5	43
88	Evaluation of Ordinary Least Square (OLS) and Geographically Weighted Regression (GWR) for Water Quality Monitoring: A Case Study for the Estimation of Salinity. Journal of Ocean University of China, 2018, 17, 305-310.	1.2	26
89	Spatiotemporal influence of temperature, air quality, and urban environment on cause-specific mortality during hazy days. Environment International, 2018, 112, 10-22.	10.0	62
90	Verification, improvement and application of aerosol optical depths in China Part 1: Inter-comparison of NPP-VIIRS and Aqua-MODIS. Atmospheric Environment, 2018, 175, 221-233.	4.1	72

#	Article	IF	CITATIONS
91	Validation of Modis Aerosol Optical Depth Over South China Sea. , 2018, , .		1
92	Aerosol Retrievals Over Bright Urban Surfaces Using Landsat 8 Images. , 2018, , .		3
93	Evaluation of Modis C6 Combined Aerosol Product at Global Scale. , 2018, , .		1
94	Estimating PM1 concentrations from MODIS over Yangtze River Delta of China during 2014–2017. Atmospheric Environment, 2018, 195, 149-158.	4.1	36
95	An Improved Highâ€Spatialâ€Resolution Aerosol Retrieval Algorithm for MODIS Images Over Land. Journal of Geophysical Research D: Atmospheres, 2018, 123, 12,291.	3.3	42
96	Multilevel Cloud Detection for High-Resolution Remote Sensing Imagery Using Multiple Convolutional Neural Networks. ISPRS International Journal of Geo-Information, 2018, 7, 181.	2.9	58
97	Characteristic and Driving Factors of Aerosol Optical Depth over Mainland China during 1980–2017. Remote Sensing, 2018, 10, 1064.	4.0	72
98	Variations of transparency derived from GOCI in the Bohai Sea and the Yellow Sea. Optics Express, 2018, 26, 12191.	3.4	25
99	Global Validation of MODIS C6 and C6.1 Merged Aerosol Products over Diverse Vegetated Surfaces. Remote Sensing, 2018, 10, 475.	4.0	50
100	Performance of the NPP-VIIRS and aqua-MODIS Aerosol Optical Depth Products over the Yangtze River Basin. Remote Sensing, 2018, 10, 117.	4.0	51
101	Validation of MODIS C6 Dark Target Aerosol Products at 3 km and 10 km Spatial Resolutions Over the China Seas and the Eastern Indian Ocean. Remote Sensing, 2018, 10, 573.	4.0	9
102	The Characteristics of the Aerosol Optical Depth within the Lowest Aerosol Layer over the Tibetan Plateau from 2007 to 2014. Remote Sensing, 2018, 10, 696.	4.0	17
103	Improving the Estimation of Daily Aerosol Optical Depth and Aerosol Radiative Effect Using an Optimized Artificial Neural Network. Remote Sensing, 2018, 10, 1022.	4.0	44
104	A New MODIS C6 Dark Target and Deep Blue Merged Aerosol Product on a 3 km Spatial Grid. Remote Sensing, 2018, 10, 463.	4.0	47
105	Automatic method to monitor floating macroalgae blooms based on multilayer perceptron: case study of Yellow Sea using GOCI images. Optics Express, 2018, 26, 26810.	3.4	36
106	High-resolution satellite aerosol optical depth retrieval and its variability over highly industrialized hotspots in the Po Valley, Italy. , 2018, , .		1
107	New customized methods for improvement of the MODIS C6 Dark Target and Deep Blue merged aerosol product. Remote Sensing of Environment, 2017, 197, 115-124.	11.0	79
108	Evaporation modelling using different machine learning techniques. International Journal of Climatology, 2017, 37, 1076-1092.	3.5	66

#	Article	IF	CITATIONS
109	Evaluation of the NDVI-Based Pixel Selection Criteria of the MODIS C6 Dark Target and Deep Blue Combined Aerosol Product. IEEE Journal of Selected Topics in Applied Earth Observations and Remote Sensing, 2017, 10, 3448-3453.	4.9	26
110	Validation of MODIS and VIIRS derived aerosol optical depth over complex coastal waters. Atmospheric Research, 2017, 186, 43-50.	4.1	33
111	A Simple and Universal Aerosol Retrieval Algorithm for Landsat Series Images Over Complex Surfaces. Journal of Geophysical Research D: Atmospheres, 2017, 122, 13,338.	3.3	44
112	Aerosol Optical Properties and Associated Direct Radiative Forcing over the Yangtze River Basin during 2001–2015. Remote Sensing, 2017, 9, 746.	4.0	32
113	Evaluation of Empirical and Machine Learning Algorithms for Estimation of Coastal Water Quality Parameters. ISPRS International Journal of Geo-Information, 2017, 6, 360.	2.9	25
114	A New Approach for Estimation of Fine Particulate Concentrations Using Satellite Aerosol Optical Depth and Binning of Meteorological Variables. Aerosol and Air Quality Research, 2017, 17, 356-367.	2.1	51
115	Aerosol Optical Depth Retrieval over Bright Areas Using Landsat 8 OLI Images. Remote Sensing, 2016, 8, 23.	4.0	89
116	Validation of MODIS 3 km Resolution Aerosol Optical Depth Retrievals Over Asia. Remote Sensing, 2016, 8, 328.	4.0	103
117	Validation of Aqua-MODIS C051 and C006 Operational Aerosol Products Using AERONET Measurements Over Pakistan. IEEE Journal of Selected Topics in Applied Earth Observations and Remote Sensing, 2016, 9, 2074-2080.	4.9	85
118	High-Resolution Satellite Mapping of Fine Particulates Based on Geographically Weighted Regression. IEEE Geoscience and Remote Sensing Letters, 2016, 13, 495-499.	3.1	126
119	Land Use Regression Models Using Satellite Aerosol Optical Depth Observations and 3D Building Data from the Central Cities of Liaoning Province, China. Polish Journal of Environmental Studies, 2016, 25, 1015-1026.	1.2	6
120	Evaluation of MODIS aerosol retrieval algorithms over the Beijingâ€Tianjinâ€Hebei region during low to very high pollution events. Journal of Geophysical Research D: Atmospheres, 2015, 120, 7941-7957.	3.3	103
121	Validation and accuracy assessment of a Simplified Aerosol Retrieval Algorithm (SARA) over Beijing under low and high aerosol loadings and dust storms. Remote Sensing of Environment, 2014, 153, 50-60.	11.0	80
122	A Simplified high resolution MODIS Aerosol Retrieval Algorithm (SARA) for use over mixed surfaces. Remote Sensing of Environment, 2013, 136, 135-145.	11.0	143
123	Application of snowmelt runoff model for water resource management. Hydrological Processes, 2011, 25, 3735-3747.	2.6	69
124	Effects of convective available potential energy, temperature and humidity on the variability of thunderstorm frequency over Bangladesh. Theoretical and Applied Climatology, 0, , 1.	2.8	5
125	Summer Monsoon Rainfall Variations and its Association with Atmospheric Circulations Over Sudan. SSRN Electronic Journal, 0, , .	0.4	0